SSA Experiments for the Australian M2 Formation Flying CubeSat Mission

Melrose Brown, Brenton Smith, Christopher Capon, Rasit Abay, Manuel Cegarra Polo, Steve Gehly, George Bowden, Courtney Bright, Andrew Lambert, Russell Boyce
University of New South Wales Canberra, Northcott Drive, Canberra, ACT 2600, Australia

ABSTRACT

UNSW Canberra has a program of experiments onboard the M2 formation flying CubeSat mission to provide truth data for available space situational awareness (SSA) sensors and modelling algorithms. The paper outlines the program of experiments and deployments planned throughout the early, main, and extended operation phases of the mission that provide opportunities for SSA observations. The mission comprises 2x6U CubeSats. Each satellite uses a 3-axis attitude control system to exploit differential atmospheric drag forces between the spacecraft to control the along-track formation. The differential aerodynamic formation control enables the satellites to remain within an acceptable along-track offset to perform the main mission experiments. Several important opportunities to collect benchmark SSA data are present throughout the mission. The CubeSat pair are initially conjoined as a 12U satellite and, following a scheduled command from the UNSW Canberra ground station, will be impulsively pushed apart in the along-track direction by a spring to create a formation of 2x6U satellites. The separation of the spacecraft, followed by solar panel and antennae deployment, mark significant changes to the configuration, radar cross section, and orbit, during this early operations phase. The solar panel deployment increases the maximum frontal area of the spacecraft from 0.043 m^2 in stowed configuration to 0.293 m^2 when fully deployed. The attitudes of the spacecraft will be controlled to arrest the along-track separation of the spacecraft via the action of differential aerodynamic drag. The satellites feature GPS and attitude determination and control for accurate time, position, velocity, and attitude information, which is routinely available in the satellite telemetry.

The change detection experiments planned for the mission use the US Air Force Academy (USAFA) 0.5 m raven class Falcon Telescope Network and UNSW Canberra's 0.36 m Rowe-Ackermann Schmidt Astrograph (RASA). Photometry and astrometry from these sensors are used in combination with synthetic sensor data through application of novel machine-learning frameworks to provide estimates for the satellites' configuration status and attitude profile during the observations. The synthetic optical sensor data will be produced from an in-house high-fidelity GPU accelerated ray-tracing simulation tool that can model multiple reflections and account for complex material reflectance properties. Progress on the development of the GPU tool are presented. The latter stages of the mission investigate advanced differential aerodynamic control methodologies. The impact of sensor uncertainty and operational constraints on the accuracy of differential aerodynamic formation control manoeuvres will be analysed and quantified during the mission. A modelling and simulation framework will employ coupled ionosphere/thermosphere models with high fidelity force propagation tools to provide higher fidelity estimates of the non-conservative forces imparted on the spacecraft by the atmosphere than standard models provide. The extended mission phase contains an ambitious space environment research experiment that seeks to measure 'ionospheric aerodynamics' effects imparted on the spacecraft. The experiment has been developed from theoretical and numerical research at UNSW Canberra that studies the force created when a charged body interacts with the weakly ionized plasma in the ionosphere in LEO. The interaction is controlled from charge plates located on the extremity of the extended solar panels. The configuration and concept of operations are presented.

1. INTRODUCTION

In November 2017 UNSW Canberra Space embarked on an innovative space research and education program, enabled by $10M (AUD) funding provided from the Royal Australian Air Force. The program comprises research, engineering, and educational streams that centre on a series of increasingly sophisticated small satellite (CubeSat) missions. The educational goals focus on providing students from both defence and civilian backgrounds an interdisciplinary insight into current and emerging issues affecting modern space engineering, operations, and space situational awareness

(SSA). The educational offerings span UNSW Canberra's undergraduate, post-graduate, professional, and distance education programs. They provide Australian and international students at all stages of their career with direct access to the knowledge, skills, and experience contained within the team of professional engineers and research staff at the heart of the missions.

The satellite research and engineering streams focus on developing novel small satellite technologies to provide benchmark quality SSA research data and capability demonstration. The most recent launch in the series is the M2 Pathfinder 3U CubeSat (Fig. 1), which launched on Rocket Lab's 'Don't Stop Me Now' 12th mission from New Zealand's Māhia Peninsula on June 13 2020. M2 Pathfinder was designed, integrated, and tested over 10 months at UNSW Canberra Space facilities, with the structure, mechanisms, and most subsystems developed entirely in-house. The M2 Pathfinder satellite advances the technology readiness level (TRL) for critical communication, attitude determination and control, a reprogrammable software defined radio, and positioning and navigation subsystems that are crucial to the success of the main M2 mission, which is the focus of the work presented here.

Fig. 1: UNSW Canberra Space M2 Pathfinder 3U CubeSat, launched 13th June 2020 by Rocket Lab.

M2 (Mission 2) is the final mission in the series and is due for launch in Q1 2021. The mission extends the work begun by the M1 (Mission 1) and M2 Pathfinder missions. The M2 mission features a pair of near-identical 6U CubeSats, each with a suite of innovative on-board systems and sensors developed in-house at UNSW Canberra Space to demonstrate and develop cutting edge small satellite technology for maritime surveillance and SSA applications. M2 will feature re-programmable software defined radios, a panchromatic imager to image large maritime surface vessels, and novel on-board processing capabilities.

Complementing the main maritime surveillance mission is a strong SSA theme. The mission presents an opportunity for the Australian SSA community and international partners to validate and verify detection, identification, tracking, and characterization techniques during several phases of the mission. UNSW Canberra's research will use the telemetry downlinked from the spacecraft as a truth source to benchmark and explore the performance of our ground-based optical and radio frequency (RF) sensors combined with simulation tools to detect change in the orbit, physical configuration, and attitude of the pair of 6U CubeSat spacecraft.

The paper begins by defining the main M2 spacecraft geometry and briefly outlining the main on-board systems. The mission phases that provide opportunities for collaborative ground-based SSA research are presented, followed by a description of the UNSW Canberra SSA research activities associated with the mission.

2. M2 SPACECRAFT DEFINITION

The M2 mission features a pair of near-identical 6U Cube Satellites that shall orbit in formation during the main mission operations. The satellites are initially conjoined, with the complete system adhering to a 12U Cube Satellite form factor (nominally 300x200x200 mm). The form factor for the two satellites are created through bisecting the 12U form factor along the 300 mm dimension to create a pair of 150x200x200 mm spacecraft, creating a non-standard 6U form factor (Fig. 2). The configuration is advantageous for accommodating the main telescope assembly within

the chassis.

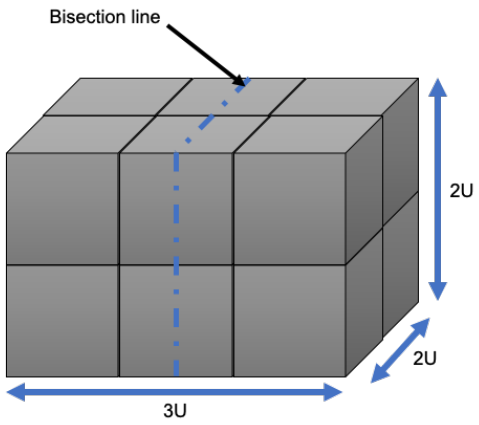

Fig. 2: The initial 12U form factor bisects into a pair of 1.5Ux2Ux2U CubeSats.

The spacecraft in its stowed 12U and separated/deployed 6U configuration is shown in Fig. 3. The satellites are joined along the Z = 0 mm face. The separation occurs after a commanded burn wire action, when the spacecraft are separated by a small spring between the spacecraft that imparts a delta V of approximately 0.01 ms^{-1}. Each 6U satellite deploys solar arrays from the ±X and ±Z faces. The ±Z solar panels feature a double-deployable solar panel mechanism. The inner panel comprise standard solar cells, however the outer panel host the charge plates for the ionospheric aerodynamic experiments conducted later in the mission (coloured orange in Fig. 3). In its fully deployed configuration, the satellite has a maximum surface area of 0.293 m^2 on the -Y face and a minimum area of 0.043 m^2 on the +X face. Each 6U satellite has a mass of 10.0 kg.

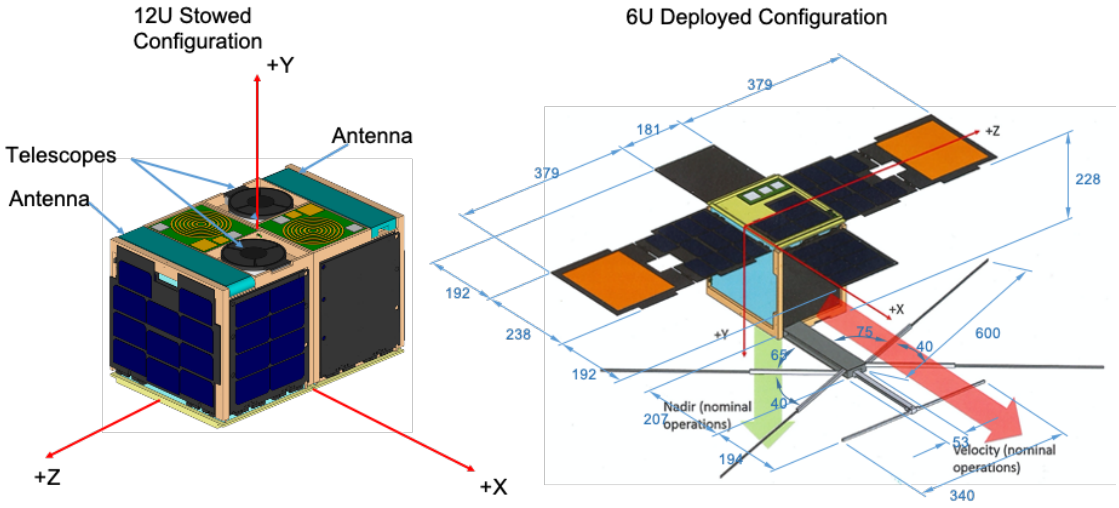

Fig. 3: The M2 spacecraft pair in 12U stowed configuration and dimensions for the 6U single satellite deployed configuration. Dimensions in mm.

The satellites will be placed into a near-circular orbit and will be launched under a ride-share agreement. The nominal orbit parameters are subject to change at this time and will become available closer to the launch, however the system is expected to operate around 500 to 550 km altitude. Reaction control wheels, magnetometers, sun and earth horizon sensors provide attitude determination and control around all three axes. Accurate position and timing is delivered through a GPS payload to supplement the on-board computer clock.

The satellites are controlled via the UNSW Canberra Space web-based mission operations and control capability

'OpsToolkit', which was designed by and for our operators to make spacecraft operations safe, efficient, and user-friendly. With appropriate credentials, the application can be accessed from any device with an internet connection, which means our operators are not restricted to working from a dedicated control room. Operations are supported by the Yass node of the UNSW Canberra ground station network, which is located just outside of Canberra and hosted by Cingulan Space. Robust communications are provided through omni-directional ultra high frequency (UHF) antennae, with higher data rates for payload data communicated to ground using an S-band link.

3. M2 MISSION PHASES FOR SSA

3.1 Launch

Launch activities inherently require SSA to ensure safe passage for the rocket system and insertion of the payloads into the desired orbit, Ride-share launches feature an increasing number of secondary payloads, and initial orbit determination and unique identification of the deployed satellites is a pressing challenge facing the community. These activities are traditionally serviced using radar and optical sensors. The program of missions has developed LED beacon technology to investigate the viability of the technology for satellite identification. The LED beacon technology demonstration on the M2 and M2 Pathfinder missions feature as possible mission extension activities and also form part of the ionospheric aerodynamics experiment, outlined in Section 6.

UNSW Canberra has also embarked on a tangential area of SSA research related to launch activity that seeks to understand and simulate the impact that rocket launches have on the ionosphere. The research is motivated by the $\sim$900 km diameter hole created in the ionosphere by the FORMOSAT-5 launch on 24th August 2017 [8] that persisted for several hours after launch. Such interactions pose the risk to disrupt the provision of communications and precise position, navigation, and timing. The research completed to date marks the first example of a space environment simulation framework to predict the ionospheric depletion caused by the interaction of rocket chemical plumes with the atmosphere during ascent. Details of the modelling approach can be found in [5]. The work shall continue through 2021. Validation activities shall compare space-based measurements of the change in the ionosphere for the M2 Pathfinder and M2 mission launches with the simulations. The future direction of the research aims to extend the work to enable discrimination between naturally arising disturbances and launch activities in measurements of the ionosphere.

3.2 Early Operations

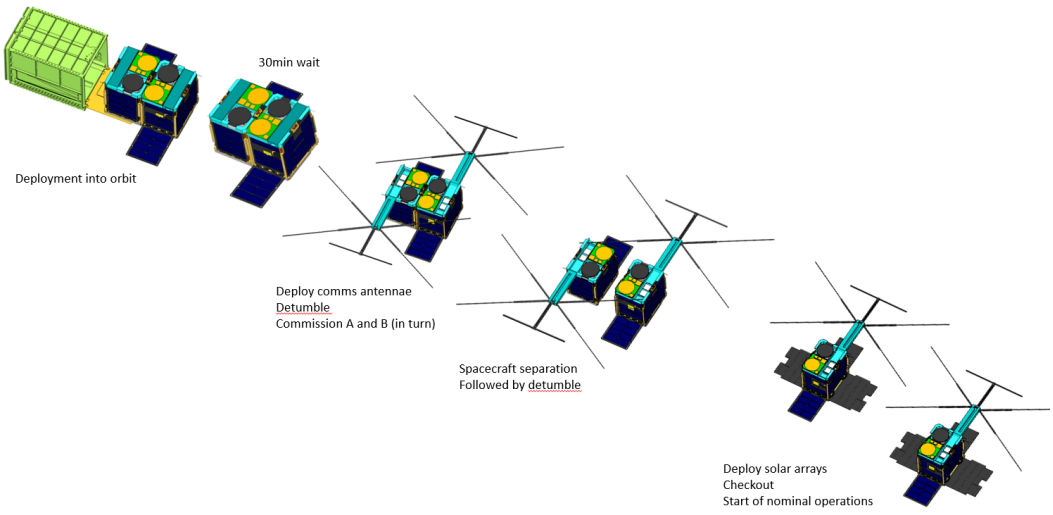

Fig. 4: Deployment and configuration changes in early operations.

The early operations phase of the mission provides several opportunities for ground-based SSA tracking and change detection activities. A nominal concept of operations for early operations is shown in Fig. 4. Following deployment from the dispenser, the spacecraft pair will commission the primary subsystems while remaining conjoined in the 12U

configuration. The spacecraft pair shall de-spin and align along the the velocity direction to ensure the separation velocity vector is directed in the along track direction. Following a scheduled command from the ground station, the satellites shall be released after a burn wire operation and impulsively separated along-track via a spring force between the spacecraft. The relative velocity between the spacecraft shall be of the order of 0.01 ms^{-1}. Antenna and solar panel deployment will change the cross-sectional area and reflectance properties between the stowed to fully deployed configurations.

The separation process has been studied to ensure the spacecraft do not come into contact post-separation. Aligning the separation velocity vector in the along-track direction provides the greatest miss distance. Fig. 5 summarises the results of the study conducted using UNSW Canberra's high-fidelity orbit propagator to specify the acceptable bounds for misalignment between the ideal along track velocity vector and that obtained on-orbit. In this figure, any separation angle that resulted in the spacecraft converging within 50 m was considered unsafe and is shown in red in Fig. 5. It was found that an angle as large as 56 degrees from along-track could still prevent converging relative motion coming within the collision avoidance threshold of 50 m. However, a conservative figure of ± 20 degrees in any direction from the along-track axis, as can be seen in Fig. 6, has been specified as a requirement to ensure collision free on-orbit operations, while remaining well within the tolerances of the on-board attitude control system.

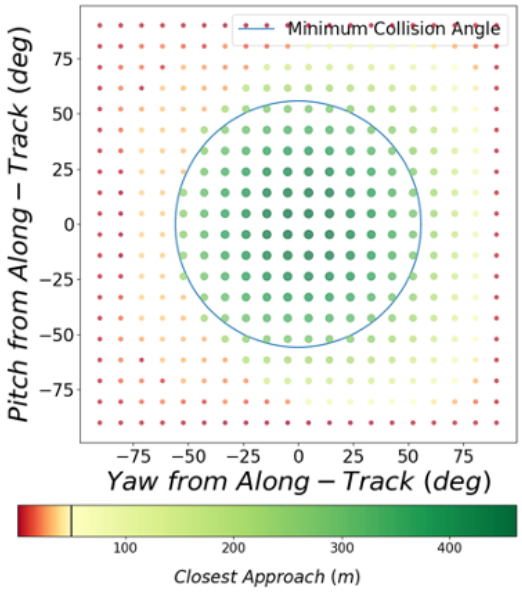

Fig. 5: Assessment of the collision risk for misaligned separation vector.

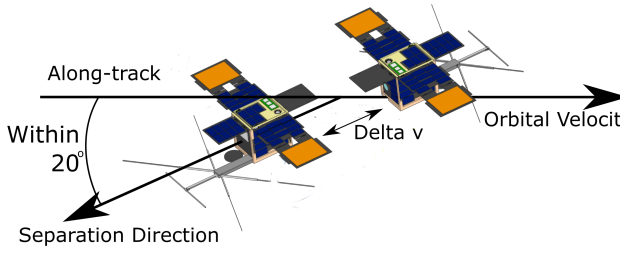

Fig. 6: Depiction of the separation angle of the spacecraft from the along-track direction.

The impulse imparted on both spacecraft by the spring during separation causes secular divergence of the spacecraft, as can be seen in Fig. 7, that if left unchecked will result in intolerably large relative distances. Therefore, stabilizing

the satellite formation is a key phase following the impulsive separation of the spacecraft. No propulsion system is included in the spacecraft bus; formation control is achieved solely through a differential aerodynamic control scheme that exploits the perturbation from atmospheric drag to provide subtle relative motion control. The details of the approach and the specific formation flying experimental objectives are detailed in Section 5. If no aerodynamic control activity is applied to arrest the separation velocity, the along-track relative offset between the spacecraft imparted will linearly increase over time. The main mission activities can commence once the relative distance between the satellites is stabilized.

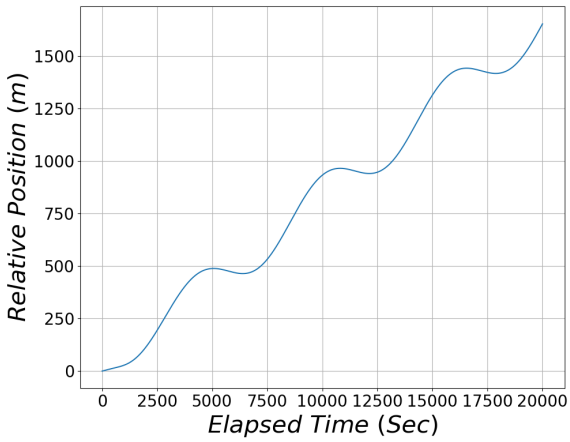

Fig. 7: Magnitude of relative position from along-track separation.

UNSW Canberra will focus on using the telemetry from M2 during this phase to advance its LEO photometry and light curve inversion research stream (Section 5). The primary objective of that research is to investigate whether numerical simulations can be intelligently combined with optical data to improve detection and characterization for increasingly subtle changes to a satellite's on-orbit trajectory and behaviour. Details of the research stream and progress with establishing the new facilities and modelling capabilities can be found in Section 4. Co-collect opportunities are being explored with partner organisations to maximize the value of the time critical and non-repeatable mission events.

3.3 Main Mission

The main mission activities commence after the satellite formation has been established and will be completed over the course of 2021. A series of technology demonstrations are performed throughout the mission lifetime, which range from advancing the technology readiness level of satellite bus subsystems through to maritime surveillance systems for ship detection using optical imaging of large surface vessels and AIS beacon detection. The design and performance of the specific on-board systems is not reported here, however, the M2 mission represents a major advance in intelligent small satellite capability development for Australia.

The differential drag aerodynamic formation control method that arrests the initial spacecraft separation, outlined in Section 3.2, is extended throughout the main mission. The formation flying experiments investigate how to operationally integrate high fidelity non-conservative force modelling and space environment simulations to improve the accuracy, precision, and time to complete small satellite formation manoeuvres. The research will provide important experience into the operational constraints and requirements of aerodynamic control for future small satellite formation missions, and provide insight into how and where aerodynamic control can be used effectively for debris avoidance manoeuvres. Section 5 details the experimental campaign. Supporting the formation flying experiments are the advances in high fidelity real-time force modelling (Section 4.4), space environment modelling (Section 4.6), and space surveillance research themes (Section 4).

3.4 Extended Mission

A number of SSA experiments are candidates for extended mission operations. Following the completion of the main mission activities, extended mission experiments can proceed, subject to budget and operational approvals. The M2

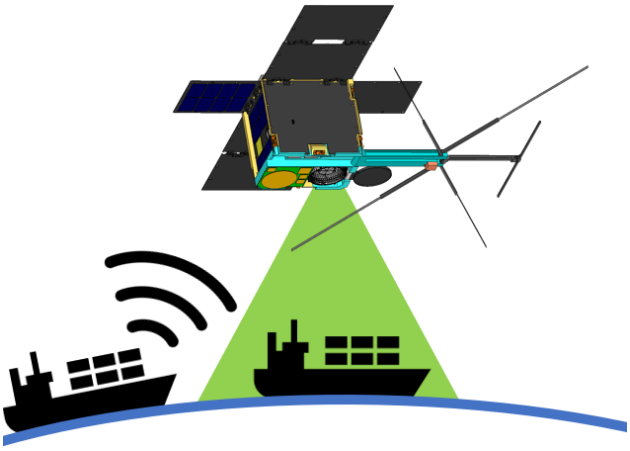

Fig. 8: M2 maritime main mission technology demonstration.

spacecraft are capable of exploring space-based space surveillance applications through re-purposing the optical and RF maritime surveillance payloads. The details of these configurations shall be reported in future publications.

A first-of-its-kind on-orbit experiment to study 'ionospheric aerodynamics' is planned for the extended mission phase. The experiment explores the additional force that charged resident space objects are predicted to experience when interacting with the weakly ionized plasma within the ionosphere. The experiment is actuated through the charge panels integrated onto the deployable solar array structures. Details of this experiment are provided in Section 6.

4. LOW EARTH ORBIT LIGHT CURVE INVERSION RESEARCH

A major SSA research theme being advanced by the M2 mission is the inversion of photometric light curves. The modern-day SSA context requires the ability to transform and synthesize data from a range of space surveillance sensors, with the goal to extract meaningful and actionable information to enable the effective management of a growing catalogue of resident space objects (RSO). Larger volumes of data can assist in achieving this goal, however, increasing the diversity of sensing modalities available to interrogate the nature of the RSO will provide a clear benefit to the process. Generating knowledge and information regarding the properties of an unknown RSO can, therefore, lead to improved object characterization and identification. Optical tracking of RSO in low Earth orbit (LEO) allows the collection of photometric light curve data through collecting a time series of non-resolved images [1]. The variation of brightness magnitude (intensity) over time is governed by a range of factors: RSO size; shape; material; body rate; phase angle between the sun, RSO, and telescope; and slant range from the telescope. The combination of all of these factors combine to produce a light curve 'signature'. The possibility to extract useful information for one or all of these properties exists through successfully inverting the measured light curve signature.

Although the light curve inversion problem is an established technique for the characterization of asteroids, artificial space objects represent a significant challenge due to their complex physical properties and attitude states [19]. The light curve inversion problem is an ill-defined problem because many parameters regarding physical properties and attitude states can be mapped to the same light curve.

Preliminary work at UNSW Canberra in 2018 used the Buccaneer Risk Mitigation Mission (BRMM) 3U CubeSat [31] as a target to generate light curves. In that work, light curves of the BRMM CubeSat (NORAD ID 43014) were obtained using 4 of the 12 nodes of the US Air Force Academy Falcon Telescope Network (FTN). The light curves were compared with low-fidelity/analytical simulated light curves using a BRDF model and attitude data downlinked from the satellite telemetry. Fig. 9 corresponds to a pass of BRMM over Colorado (US) on the 6th of June 2018. The degree of agreement between the experimental curve (blue) with the simulated one (red) is reasonable, however, differences exist. The spectral content of both curves are qualitatively similar, however, if we want to characterize the spacecraft in more detail, or train a machine-learning model, we need to pursue higher quality light curves. The principle features to improve are the temporal resolution to resolve the local maxima and minima flux values.

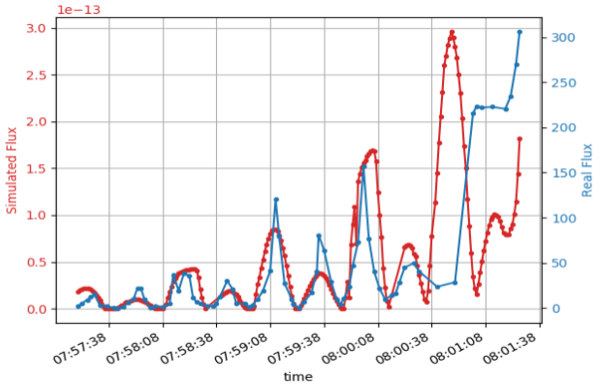

Fig. 9: Simulated and measured light curves for the Buccaneer Risk Mitigation Mission.

The research in progress for the M2 mission provide significant advances in fidelity and sophistication from the BRMM work conducted in 2018:

- The acquisition of a new optical telescope with improved sensitivity, field of view, and resolution.
- The development of a high-fidelity light curve simulation tool, utilizing state-of-the-art Graphical Processing Unit (GPU) technology, verified and validated against real photometric light curve data.
- The detailed investigation and application of cutting edge generative machine-learning methods to photometric light curve data.
- The use of real photometric light curves obtained from 3U (M2 Pathfinder), 6U (M2 deployed), and 12U (M2 stowed) nano-satellite platforms orbiting in LEO, benchmarked against attitude, position, and timing data from the spacecraft telemetry stream. The light curve data is used to train and evaluate the performance of the machine-learning framework.

The light curve inversion problem will be explored throughout the major mission phases of M2, seeking to detect, identify, and characterise the on-orbit changes that occur in spacecraft configuration, attitude, and trajectory.

4.1 Optical Space Surveillance Developments

There are several factors that influence in the quality of the experimental light curves when tracking and imaging LEO objects. The most important are the telescope field of view (FOV), the timing resolution of the light curve, the signal-to-noise ratio (SNR), exposure time and shutter mode of the image sensor, the effect of the mount when tracking high speed objects, and the effect of atmospheric turbulence. The higher the quality of the experimental light curve, the better the training subset of images that will be used in the machine-learning algorithm, and consequently the algorithm will resemble the real behaviour of the light curves more closely. Uncertainties regarding the location of LEO objects can be of the order of 1 to 5 km due to inaccuracies reported in two-line element (TLE) catalogues. If the optical ground sensor used to detect the object doesn't have a sufficiently large FOV, the telescope can miss the object on the science camera. An appropriate FOV to conduct the proposed research would be of the order of 1 to 2 degrees of sky coverage, which would guarantee that the object is always within the FOV. Astrographs are telescopes whose main characteristic is that they have a shorter focal length compared to standard telescopes. The shorter focal length allows them to image a wider region of the sky and are an appropriate choice for the proposed Space Surveillance activities. UNSW Canberra Space is currently acquiring a 36 cm Celestron RASA telescope that will provide a FOV of 1.6 x 1.6 deg.

The new wide field of view telescope includes an OTA (Optical Tube Telescope) of 36 cm (Celestron RASA36), a professional-degree mount (Paramount MX+) and a high-resolution CMOS sensor (Ximea MX120MG). These components were carefully selected with the aim for the telescope to be dedicated for SSA, with emphasis in LEO. The RASA36 telescope is arranged in a Rowe-Ackermann Schmidt configuration, which allows it to include a very short

F-number (2.2). At the focal plane, the telescope produces a 60 mm circular field of view, provided a suitably large image sensor is situated at that plane. The 4-element lens train located before the focal plane, correct for coma, false colour and field curvature. It also includes an extended spectral range that improves the image sensor response in the 700-900 nm wavelength range, leading to a higher brightness in the detected signals in the sensor.

Paramount MX+ is a high-accuracy robotic telescope mount, used in many professional-level observatories in the world. It includes the T-Point software package, currently a standard in astronomical telescopes, that can reach a high accuracy when pointing towards astronomical objects, down to a few arcseconds. The Ximea MX120MG sensor is the AMS CMOSIS CMV12000 image sensor, with 12 Mpixels resolution and a large sensor size (diagonal active area 28 mm), to take advance of the large image circle of the RASA36 OTA. The combination of the short F-number of the OTA, together with the pixel size of the image sensor, means that an unresolved object in the sky will be covered by just one pixel, increasing by a factor of 8 or more the brightness of standard F-number telescope (F/8 or F/10), which usually are affected by atmosphere turbulence effects to a greater degree. The data interface of the camera is PCI Express Gen2 (PCIe) with allows a high throughput of data out of the sensor, with in turn will have a very positive impact on the temporal resolution of the light curves, in the order of milliseconds, even for small objects such as CubeSats in LEO. The Ximea MX120MG interfaces directly with a Jetson TX2 GPU, which complements the camera for fast processing of images, that is then sent to a main external computer.

The combination of the three main components of the telescope (OTA, mount and image sensor), aimed for SSA applications, makes this apparatus a superb optical instrument for accurately tracking objects in LEO:

- A wide field of view compensate for TLE inaccuracies.
- A wide field of view allows detection of more than one object in the same image, which allows the study of constellations of satellites and is well suited for detection of M2 early operations activities and formation flying manoeuvres.
- A wide field of view combined with the optimal optics before the focal plane of the telescope allows the light to focus quickly. This compensates for atmosphere turbulence aberrations, increasing the signal-to-noise ratio in the camera by a factor of at least 8. This will increase the ability to detect smaller RSOs.
- High throughput from the camera permits high temporal resolution light curves, which leads to more accurate rotation and attitude information capture within the photometric light curve.
- The Robotic Paramount MX+ mount allows a smooth and precise tracking of objects (no leap-frog tracking), increasing the resolution and the accuracy of the photometric measurements.

Some delays have been incurred in the commissioning at the beginning of 2020 due to COVID-19. The major hardware components have been acquired, with installation and commissioning expected to be complete by the end of 2020.

4.2 Synthetic Light Curve Developments

The incorporation of realistic light curve simulation into machine-learning methodologies not only requires the ability to accurately simulate the collection of light by sensor with finite shutter speeds and exposure times as it reflects off a complex, tumbling object under realistic lighting conditions, but also requires the ability to do this very quickly. Recent advances in Graphical Processing Units (GPU) technology are making both of these capabilities possible.

NVIDIA's RTX 20 series GPU represents a step-change in computational capabilities through the introduction of their Tensor and Ray Tracing (RT) cores. Each Tensor core provides a dedicated data path custom-crafted to dramatically increase floating-point compute for matrix operations. These cores alone have enabled an 12x speed-up in throughput for machine-learning applications. The RT cores on the other hand, represent a new dedicated compute pathway optimised for ray-tracing applications, which effectively requires the rapid calculation of intersections between a line (ray) and object primitive (e.g. triangle) stored inside a Bounding Volume Hierarchy (BVH) data structure. This optimized pipeline has led to a dramatic uptick in RT capabilities, with the GTX 1080 Ti capable or approximately 1.2 GigaRays/second vs the equivalent RTX 2080 Ti GPU capable of 10 GigaRays/second. It is the combination of the Tensor and RT cores that has enabled NVIDIA to achieve milestone previously thought unattainable in the games industry, real-time ray-tracing. It is also this combination of technologies that this project seeks to leverage to provide realistic light-curves of complex objects at speeds fast enough to support machine-learning systems through the virtual training methodologies.

The standard application of ray-tracing for rendering involves casting a large number of rays from the a desired view point, rapidly determining the intersection of these rays with objects and modifying an attached data structure by sampling some interaction function e.g. a bidirectional reflectance distribution functions (BRDF). Rays are then recursively propagated until their meet a termination criterion. Examples of termination criteria are not calculating intersections with an object in the scene (miss), maximum number of recursions reached (catch infinite recursions, reduce computational load) or ray connects with a light source. For the last case, the ray data structure attached to the ray that holds a history of its interaction with objects is stored as a confirmed hit on the pixel array, which may be then used to render an object.

These workflows, along with more complex RT techniques (shadow rays, motion blur, etc.) not discussed here, are identical to simulating the response of a light-based detector. For example, Wilkman [49] applied RT techniques to simulate the detector signal in a Satellite Laser Ranging (SLR) system. Given a known transmission pulse rate, Wilkman simulated the time-varying response of an SLR detector to a range of increasingly complex, tumbling objects. A key result from there work was to demonstrate that simulated detector response of each object contained underlying characteristic features. These features, though complex, could be used to train a machine-learning network to determine properties about the observed object e.g. shape, attitude, body rates. This work proposes to extend the work of Wilkman [49] by developing the ability to rapidly construct virtual light curves of complex, tumbling objects using realistic BRDF models and directly modelling known sensors using next-generation RT capabilities. Through an iterative process of cross-comparison and improvement of virtual light curves with the collected light curves of known objects, this work will aim to develop the capability to rapidly and realistic simulate light curves of complex objects which can them to used to expand the training dataset of machine-learning models, with the goal of increasing their ability to infer properties of unknown objects through inversion of their light curves.

The RayMAN simulation tool has advanced significantly over the course of 2020. Fig. 10 shows the output from an example simulation sweep. The M2 spacecraft CAD is natively read into the system, which virtually eliminates pre-processing time. Rays are cast from the sensor out towards the satellite. The rendered image is shown in the main figure to indicate the lighting condition. The result in the bottom right of the figure shows the variance in light intensity recorded on the simulated sensor for a range of attitude conditions. RayMAN development is proceeding and shall include full light curve reconstruction for M2 passes over the new telescope facility by early 2021.

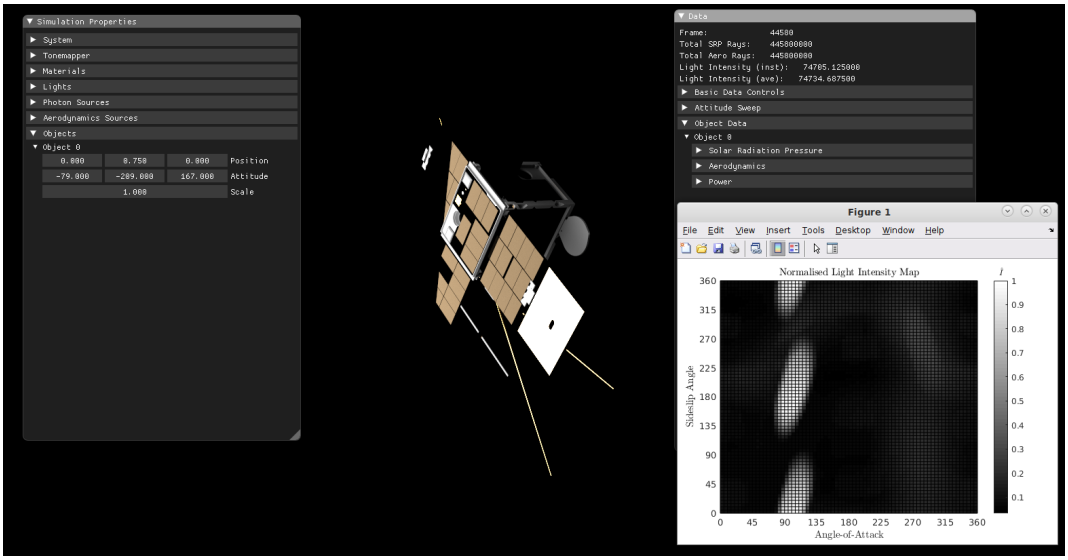

Fig. 10: Preliminary results from the RayMAN synthetic light curve simulation tool.

4.3 Machine-Learning Framework Concept

The amount of data to be processed for SSA are increasing due to the new launches and SSA sensors that are being deployed. Computationally efficient algorithms that can address the imminent data deluge in SSA are desired. Current practices in catalog maintenance rely on the simplification of the physical properties of RSOs to primitive

shapes such as 'cannonball', and catalog objects with simple coefficients, such as air drag and solar radiation pressure coefficients. This simplistic approach in the characterisation of RSOs limits the dynamical models to predict the future states accurately. Light curves are sensitive to shape, size, attitude, angular velocity, and surface properties of space objects. The state-of-the-art methods for characterising RSOs, namely nonlinear state estimation, multiple models, and full Bayesian inversion, are compute-intensive methods, and they are not efficient for larger volume of data because each process needs to be repeated without gaining any experience. In addition, light curve inversion problem is an ill-posed problem, and machine-learning can be leveraged to characterise and identify RSOs more accurately and computationally efficiently. A more realistic definition of the characteristics of RSOs in the catalogs will improve the understanding of the their behaviour in orbit. The developed machine-learning framework will also segue into autonomous characterisation and identification of RSOs in near real-time.

The machine-learning framework is intended for mapping light curves to the realistic characteristics of RSOs. The research seeks to discover the factors that constrain the accuracy of a given measured light curve and associate these indicators as meta-data with each light curve to improve the performance of the machine-learning frameworks. Hybrid machine-learning frameworks are being studied to blend generative and discriminative models with classical statistical methods. Through an iterative process of data collection, validation and analysis, these frameworks will be rigorously tested and compared against known light curves of known objects and ray-tracing based BRDF simulation methods to maximize the inference capabilities of the trained models. The developed machine-learning framework seeks to address 3 challenges in using machine-learning for light curve inversion:

- 'Closing the reality gap': Generative machine-learning algorithms will be applied to assess whether simulated light curves can be modified to reflect the realistic noise, bias, and errors arising in observed light curves. The approach will use observed light curve data associated with known spacecraft attitude states from telemetry downlink to train and validate the method. The meta-data derived during stream 1 shall be included within the study to determine its effect on the correlation of the data. Successfully 'closing the reality gap' will reveal important information regarding the mapping between simulated and observed light curves and provide the potential to improve the performance of machine-learning frameworks through enhanced realism of the training data.
- Isolated light curve study: Assuming no a priori knowledge of the RSO, we will investigate and optimize hybrid machine-learning architectures to maximize the amount of information that can be extracted from data contained within isolated light curves. In addition to the systematic study of the algorithmic elements comprising the hybrid machine-learning framework, the sensitivity of the models to the volume, structure, and form of the training data will be fully explored. A key outcome will be the quantification of the assumed advantage that including observed light curve data provides to the performance of the framework. The light curve meta-data shall be further explored to determine the extent to which it can predict light curve quality.
- Multiple light curve study: The methods shall be extended to investigate whether multiple light curves can be used to derive a more accurate estimates of RSO properties than a single, isolated, light curve can provide. Light curves from a single sensor that has obtained data from successive passes; multiple sensors operating in parallax mode (i.e. observing the same RSO synchronously), and multiple sensors observing the same RSO asynchronously (i.e. different nodes of the Falcon Telescope Network that image an RSO during the same pass) shall be studied to understand how generative methods can exploit multiple data sources to contextualize data to provide improved state estimates. An extension to this phase of the work involves using this approach to predict the optimal sensor-tasking schedule to reveal the maximum information about an RSO with the minimum number of observations.

4.4 High Fidelity Force Modelling

In the recent satellite aerodynamic literature, there has been a general focus on application of particle-type methods, such as Direct Simulation Monte Carlo (DSMC). The principle advantage of DSMC methods is the ability to capture particle-particle collisions in rarefied flows, which is particularly important for vehicles between 100 to 150 km altitude. As altitude increases, however, the system quickly transitions to free molecular flows (FMF), where there are effectively no particle-particle collisions in the frame of standard LEO objects—the International Space Station being the main exception. As such, for a majority of LEO objects, perturbation modelling from an aerodynamics and solar radiation pressure (SRP) perspective reduces to a surface interaction problem, where a phenomenological model

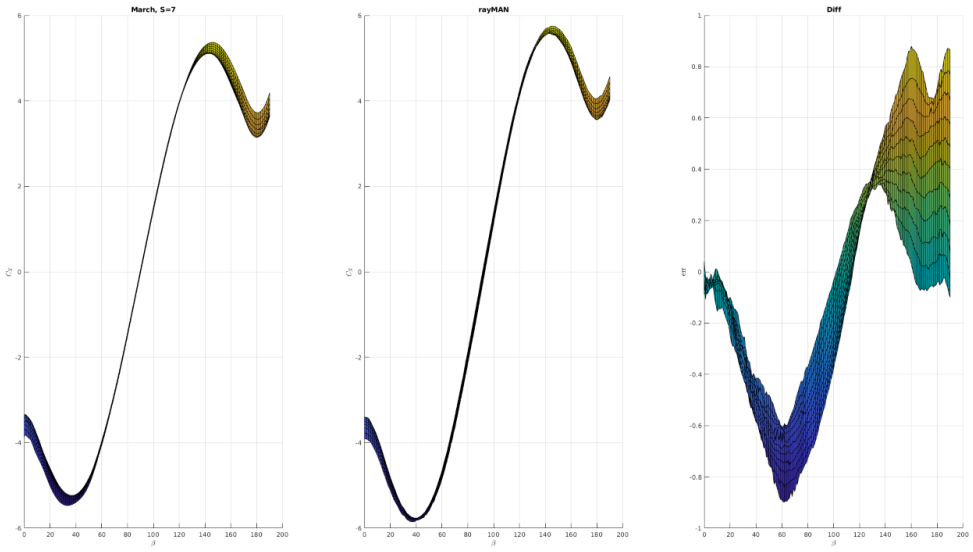

Fig. 11: Comparison between SWARM-C C_X for a fixed speed ratio $S = 7$ predictions March (left), RayMAN (middle) and differences (right).

may describe the re-emission pattern and characteristics of a photon or gas particle. Complexities then arise from the distribution of surface interaction models over an object, the variation of surface properties with time, the ability to resolve surface geometries accurately, and capturing the effects of multiple reflections by a single species. This makes the system particularly suited to modelling through ray-tracing methods.

As introduced previously, RayMAN (Ray Modelling and Analysis tool), is an in-house GPU-accelerated ray-tracing code built using NVIDIA's OptiX API [26]. Figure 4.4 provides a high-level overview of RayMAN's structure. In brief, RayMAN employs a recursive path tracing method to rapidly calculate solar radiation pressure and aerodynamic forces. Complex CAD objects are imported and stored on GPU devices (devices) in logical space. Objects are then instanced from these stored geometries and assigned an instanced material program (also stored device side). Ray interactions are rapidly calculated using an in-built accelerated Bounding Volume Hierarchy (BVH) method tailored for NVIDIA's RTX units to rapidly and efficiently calculate intersection with objects. This approach allows complex scenes of geometries with high levels of detail and low memory overheads. Upon an intersection of a ray with an object, the associated material program linked with the object is called based on the incident ray type - radience, aerodynamic or photon. Material programs update ray properties based on interaction models. RayMAN handles an arbitrary number of different material types with variable interaction properties for different ray types, e.g. diffuse reflection for aerodynamic rays and specular reflection for solar radiation pressure rays. This allows rapid investigations of gas/surface interactions with complex variation in surface properties.

Instead of a pixel array method, such as that described by Li et al. [21], RayMAN fills a pre-allocated device-side hash table of ray interactions which are then copied to the host machine after each cast to minimise copy operations. The copied ray path table is then accumulated on an object mesh, providing a robust link between ray interactions and object geometry. Aside from reducing copy overheads, this approach enables multi-object simulations and the interaction of multiple ray types. For example, work underway is to link an in-house thermal solver with RayMAN to provide accurate thermal view factors while also calculating variations with local surface temperature and therefore forces from re-emitted gas particles. RayMAN also includes a ray-tracing based visualisation mode using OpenGL with interactive controls built using imgui that allows dynamic reassignment of material programs to surfaces, aerodynamic and solar radiation pressure source profiles and object position and attitude. Figure 4.4 shows a work-in-progress comparison between RayMAN and the aerodynamic data table provided by TU Delft [18] for the SWARM-C satellite calculated using SPARTA-DSMC. With no optimization, RayMAN reproduced these 2100 datapoints in 25 minutes ($<$ 1 data point/second) with a reasonable level of accuracy. Current work is investigating potential sources of difference in gas/surface interaction model and particle seeding approaches to improve agreement.

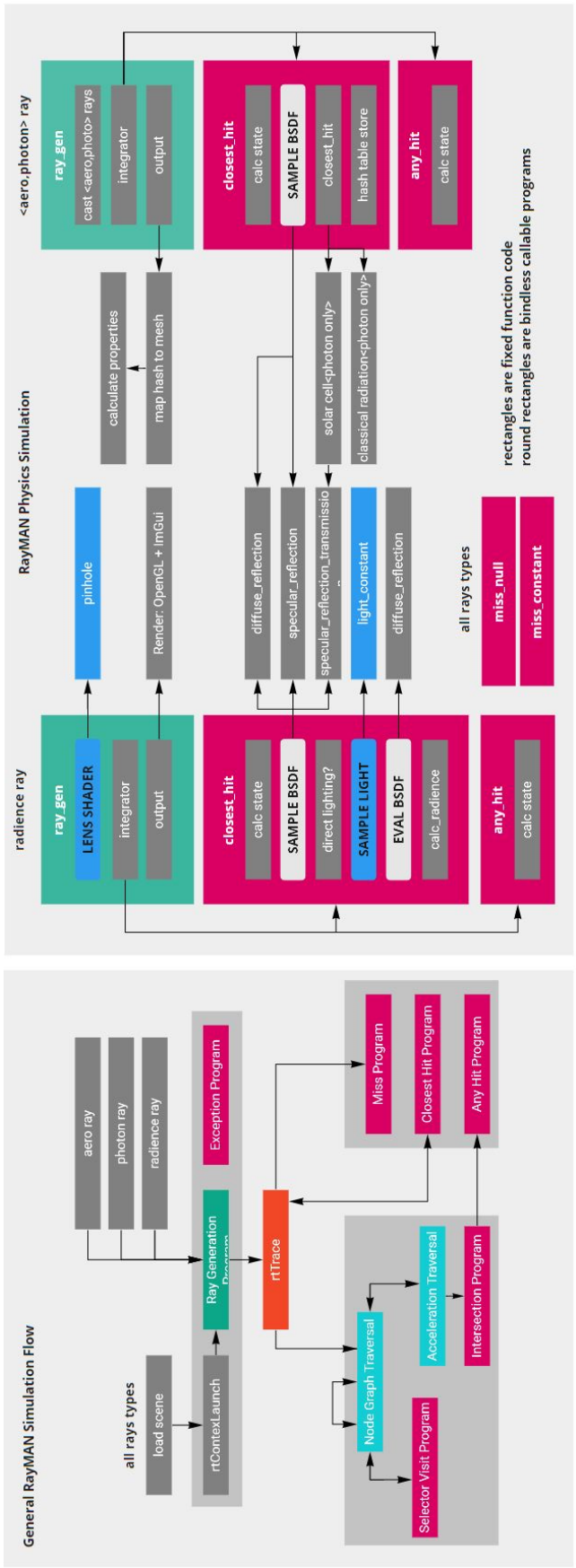

Fig. 12: High-level overview of RayMAN implementation.

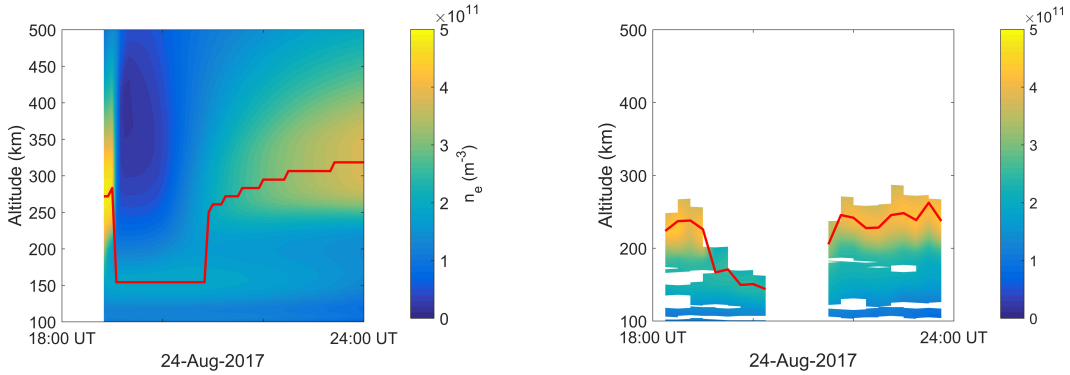

(a) GITM simulation (b) Ionosonde data

Fig. 13: Comparison between electron number density profiles and peak altitudes (red lines) obtained (a) from GITM numerical modelling and (b) from the Point Arguello ionosonde at (33°36′ N, 120°36′ W) following the FORMOSAT-5 launch, reprinted with permission from Bowden et al. [5].

4.5 Space Environment Modelling

To better estimate the effect of neutral aerodynamic forces on the M2 satellites in an operational context, a localised density prediction approach will be used. In this approach, a function is derived which predicts the densities encountered by a particular spacecraft using those measured previously as input. Such methods have previously been described by Stasny et al. [42], who used a linear autoregressive model, and Perez et al. [29], who used an artificial neural network. Neutral mass density will be predicted along the orbits of the M2 satellites based on previous measurements of this quantity based on precise orbit determination using GPS data and high fidelity force modelling. The prediction models will also incorporate additional information regarding the thermosphere state in the form of space weather indices; namely time series for $F_{10.7}$, a proxy for extreme ultraviolet flux, and a_p, describing geomagnetic activity.

The local density prediction approach will be compared with the use of an empirical model, NRLMSISE-00 [30], and a physical model, TIE-GCM [32]. Predictions of the space weather indices used to drive these models will be made based on artificial neural network derived forecasts. Moreover, TIE-GCMl will be run assimilating neutral mass density data from the spacecraft using an Ensemble Adjustment Kalman filtering scheme implemented through the Data Assimilation Research Testbed [2]. This follows an approach to thermosphere mass density estimation described by Matsuo et al. [23].

4.6 Sensing Launch With the Ionosphere

The launch of the spacecraft also provides an opportunity to study related impacts on the ionosphere. If the trajectory of the launch vehicle were approximately known, the depletion of the ionosphere by rocket exhaust gasses can be modelled using a modified version of the Global Ionosphere Thermosphere Model (GITM) developed at UNSW Canberra Space [5]. Such modelling may be compared with ionosonde, satellite navigation signal delay, and satellite-based Langmuir probe measurements in the region surrounding the launch site. An example of a comparison between this numerical modelling and ionograms is shown in Fig. 13. This comparison may offer insight into impacts of rocket launches on satellite navigation and high frequency radio communications in addition to chemistry and transport processes within the coupled ionosphere-thermosphere system.

5. FORMATION FLYING

The M2 mission will progress the state-of-the art of propellantless satellite formation flying in LEO. As one of the first miniaturised satellite formation missions flown by an Australian-based organisation, the M2 mission will increase the capability and heritage of satellite formation flying operations within Australia, centred at UNSW Canberra Space.

The M2 mission will advance the state-of-the-art in aerodynamically actuated satellite formation flying by increasing the accuracy of space environment forecasting and their subsequent perturbing effect on the spacecraft. These space environment modelling will then be implemented within satellite formation control algorithms that will test the precision of satellite formation manoeuvres through a series of in-orbit experiments.

5.0.1 Formation Flying Experiments

Many new space entities require a multitude of spacecraft operating in controlled formation to deliver sought-after space-derived products and services. For example, the commercial entity, Planet Labs uses differential drag to phase dozens of spacecraft within a single orbital plane to provide sufficient Earth coverage to offer insights about the globe from daily updated Earth imagery [11]. Additionally, some missions require multiple spacecraft to operate in formation to enable their primary mission objectives such as for quantum communications [25]. The agile space philosophy adopted by many miniaturised spacecraft operators emphasises simplicity of design to enable rapid design, development, launch, and operation cycles. This often results in miniaturised spacecraft designs that opt to use differential aerodynamics to actuate satellite relative motion. Differential aerodynamics requires the identical spacecraft to mismatch their cross-sectional area through changes in attitude, as shown in Fig. 15 or to deferentially electrically charge the spacecraft [41]. Nasa's CYGNSS constellation used differential drag via attitude mismatches to establish and maintain the phase eight spacecraft provide sufficient Earth coverage to monitor hurricanes [6]. Coplanar phasing of spacecraft involves setting and maintaining the difference in mean argument of latitude of the spacecraft which are otherwise in the same orbit, as shown in Fig. 14. Coplanar phasing of spacecraft is a very common manoeuvre for miniaturised spacecraft launched in a near-same orbit by a single launch vehicle [38]. As is typical of satellite formation flying missions, the uncertainty in the atmospheric density and satellite aerodynamic coefficients of the CYGNSS satellites limited the precision of relative motion that could be achieved [6]. Adaptive control techniques have been proposed in the literature to compensate for atmospheric density uncertainties [27], however, most adaptive aerodynamic satellite formation control algorithms in the literature do not account for the need to account for primary mission objectives, anomalous faults, and other operational needs such as power generation during manoeuvring, such was the case for CYGNSS and for all satellite formation operations.

The M2 formation flying experiments seek to demonstrate increased precision, robustness, and autonomy of novel aerodynamically-actuated formation flying algorithms that will pave-the-way for future formation flying capability.

The M2 mission will do this in the following ways:

1. Demonstrate precise long-term coplanar phasing of the M2 spacecraft through adaptive control algorithms that compensate for uncertainties in atmospheric density estimations and thus enable stable and accurate long-term control of satellite relative motion. These adaptive control algorithms will be complemented with more accurate atmospheric density prediction techniques, through the use of numerical models such as GITM, coupled with

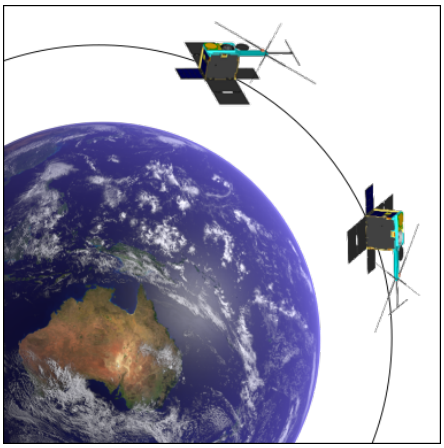

Fig. 14: Demonstration of coplanar phasing of the M2 spacecraft.

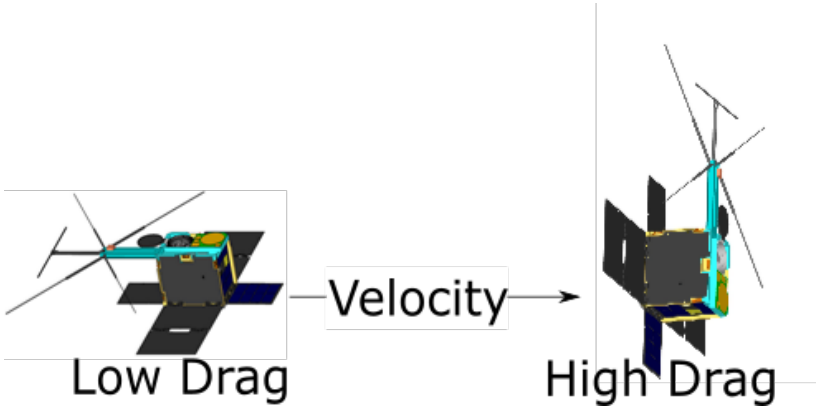

Fig. 15: Cross-sectional area mismatches causing differential drag.

machine-learning regression and calibration models based on those by Perez et al. [29, 28]. The combination of the above techniques will facilitate satellite formation control seeks to push the boundaries of precision for aerodynamically actuated satellite formation control.

2. Increase automation of satellite formation operations taking into account primary mission and operational constraints. Such capability will be achieved through a combination of rules, optimisation, and reinforcement learning techniques [37].

3. Validate on-orbit that differential aerodynamic lift can be used to actuate changes in components of relative motion normal to the orbital plane of the spacecraft. Such a capability is beneficial because differential drag alone cannot control components of relative motion normal to the orbital plane of the formation flying spacecraft [40]. Despite formation flying control algorithms existing in the literature [40, 17, 45], to the knowledge of the authors, no spacecraft has demonstrated such capability in space. Further experiments will seek to verify that differential lift can be used in combination with differential drag to actuate relative motion about all three translational degrees of freedom simultaneously or in sequence, as was described by Smith [36].

Aerodynamically-actuated satellite formation flying manoeuvres require sufficient control authority from aerodynamic accelerations to adequately actuate satellite formation flying manoeuvres. This is particularly the case for differential lift accelerations, which can be an order of magnitude smaller than differential drag, itself a very subtle acceleration. Therefore, the satellite formation flying experiments will be conducted in the later phases of the mission where the atmospheric density, and therefore, the aerodynamic acceleration will be larger because the M2 spacecraft will orbit at lower altitude due to their orbit decay.

6. IONOSPHERIC AERODYNAMICS EXPERIMENTS

The study of plasma-body interactions in LEO has historically been focused on characterizing plasma wake structures, where numerical [48, 20, 47, 22, 46] and experimental [15, 43] predictions have been supported by a limited number on-orbit missions in LEO, such as CHAWS [9, 10]. Several reviews on the subject can be found within the literature [14, 12, 13], the primary driver being to develop a better understanding of spacecraft charging and related electrostatic discharge/arcing events with recent works considering multi-body charging problems and LEO charging [47, 24, 3, 4]. As discussed in previous sections, there is a growing interest within the industry to leverage space environment interactions, such as aerodynamics, for passive spacecraft control. Following a similar theme, a number of mission concepts have been proposed that might take advantage of the electrical interaction between LEO objects and the Earth's electromagnetic environment. Perhaps most well known in this category are 'Lorentz' type missions, such as electrodynamics tethers that induces forces as a result of a charged satellite moving through the Earth's magnetic field [16, 44]. Less well known are 'Coulomb' type missions that aim to control the direct electrostatic interaction between a plasma and an embedded object. Two examples within the literature are the E-Sail payload on the ESTCube-1 [33] and the touchless actuation proposal by [34] for GEO spacecraft.

The 'Ionospheric aerodynamic EXperiment' (IEX) aims to take world-first on-orbit measurements of forces that result from the direct interaction between the ionosphere and LEO objects. IEX will develop our fundamental understanding of momentum exchange processes that result from plasma-body interactions. These results will have a range of implications:

1. **Thermospheric Models:** Ionospheric aerodynamic perturbations are hypothesised to contribute to systematic over-predictions of neutral density by empirical thermospheric models in recent work by Capon et al. [7].
2. **Coulomb Technologies:** An improved understanding of plasma aerodynamics will support the development of electromagnetic actuation technologies. For example, Smith et al. investigates the use of ionospheric aerodynamics to actuate satellite formation control [39] and to accelerate deorbit from upper LEO [35].
3. **Operations:** A better understanding of plasma-body interactions will improve orbit prediction and determination capabilities, while informing charge control strategies during space weather events.

7. CONCLUSION

UNSW Canberra's M2 mission features a sophisticated pair of 6U CubeSat spacecraft. The mission offers opportunities to explore and benchmark SSA sensors and high fidelity simulation models to detect, identify, and characterize the aerodynamically controlled formation in LEO. Several streams of research are involved with the mission, including photometric light curve inversion, sensing launch through rocket plume interaction with the ionosphere, aerodynamic actuated formation flying concepts, and a first-of-its-kind on-orbit experiment to measure the drag force produced when charged bodies orbit within the ionosphere. The M2 mission represents a major advance in capability and technical demonstration for Australian intelligent small satellite research and design. The technical advances made during the program of missions are directly informing the Australian space education and training activity across undergraduate, postgraduate, and professional development education offerings.

8. ACKNOWLEDGEMENTS

The research conducted within the program has been made possible through significant funding provided from the Royal Australian Air Force (RAAF) and internal strategic funding by UNSW Canberra. The Asian Office of Research and Development (AOARD) has provided a series of grants that have enabled the fundamental research central to the ionospheric aerodynamics experiments and associated modelling and simulation developments. The numerical work has been supported through the National Merit Computational Access Scheme and used the Raijin and Gadi high performance computing resources at the National Computing Institute.

9. REFERENCES

[1] JL Africano and T Schildknecht. International geostationary observation campaign. *Inter-agency space debris coordination committee (IADC) report AI*, 12, 2000.

[2] Jeffrey Anderson, Tim Hoar, Kevin Raeder, Hui Liu, Nancy Collins, Ryan Torn, and Avelino Avellano. The data assimilation research testbed: A community facility. *Bulletin of the American Meteorological Society*, 90(9):1283–1296, 2009.

[3] Alexander Barrie. *Modeling Differential Charging of Composite Spacecraft Bodies Using the Coliseum Framework*. PhD thesis, Virginia Polytechnic Institute, 2006.

[4] Grant Bonin, Nathan Orr, Robert E Zee, and Jeff Cain. Solar Array Arcing Mitigation for Polar Low-Earth Orbit Spacecraft. In *24th Annual AIAA/USU Conference on Small Satellites*, 2018.

[5] George William Bowden, Philippe Lorrain, and Melrose Brown. Numerical simulation of ionospheric depletions resulting from rocket launches using a general circulation model. *Journal of Geophysical Research: Space Physics*, 125(6):e2020JA027836, 2020.

[6] Charles D Bussy-virat, Aaron J Ridley, Abhay Masher, Kyle Nave, and Marissa Intelisano. Assessment of the Differential Drag Maneuver Operations on the CYGNSS Constellation. *IEEE Journal of Selected Topics in Applied Earth Observations and Remote Sensing*, 12(1):1–9, 2019.

[7] C. J. Capon, B. Smith, M. Brown, R. Abay, and R. R. Boyce. Effect of ionospheric drag on atmospheric density estimation and orbit prediction. *Advances in Space Research*, 63(8):2495–2505, 2019.
[8] Min-Yang Chou, Ming-Hsueh Shen, Charles CH Lin, Jia Yue, Chia-Hung Chen, Jann-Yenq Liu, and Jia-Ting Lin. Gigantic circular shock acoustic waves in the ionosphere triggered by the launch of formosat-5 satellite. *Space Weather*, 16(2):172–184, 2018.
[9] V.A. Davis, M.J. Mandell, D L Cooke, and C L Enloe. High-voltage interactions in plasma wakes: Simulation and flight measurements from the Charge Hazards and Wake Studies (CHAWS) experiment. *Journal of Geophysical Research*, 104(A6):12,445–12,459, 1999.
[10] C L Enloe, J T Bell, D L Cooke, D. A. Hardy, J W R Lloyd, and M D Violet. The Charging Hazards and Wake Studies (CHAWS) Experiment. In *33rd Aerospace Sciences Meeting and Exhibit*, 1995.
[11] Cyrus Foster, James Mason, Vivek Vittaldev, Lawrence Leung, Vincent Beukelaers, Leon Stepan, and Rob Zimmerman. Constellation Phasing with Differential Drag on Planet Labs Satellites. *Journal of Spacecraft and Rockets*, 55(2):1–11, 2017.
[12] Henry B Garrett. The charging of spacecraft surfaces. *Review of Geophysics*, 19(4):577–616, 1981.
[13] Henry B. Garrett and Albert C. Whittlesey. Spacecraft charging, an update. *IEEE Transactions on Plasma Science*, 28(6):2017–2028, 2000.
[14] D. E. Hastings. A review of plasma interactions with spacecraft in low Earth orbit. *Journal of Geophysical Research*, 100(A8):14457–14483, 1995.
[15] S. D. Hester and Ain. A. Sonin. A laboratory study of the electrodynamic influences on the wakes of ionospheric satellites. *2nd Fluid and Plasma Dynamics Conference*, 8(6):1090–1098, 1969.
[16] Robert Hoyt. Terminator Tape: A Cost-Effective De-Orbit Module for End-of-Life Disposal of LEO Satellites. *AIAA SPACE 2009 Conference & Exposition*, (September):1–9, 2009.
[17] D. Ivanov, M. Kushniruk, and M. Ovchinnikov. Study of satellite formation flying control using differential lift and drag. *Acta Astronautica*, 152(March):88–100, 2018.
[18] E. Iorfida G. March C. Siemes O. Montenbruck J. van den IJssel, E. Doornbos. Thermosphere densities derived from Swarm GPS observations. *Advances in Space Research*, 2020.
[19] Mikko Kaasalainen, Johanna Torppa, and Karri Muinonen. Optimization methods for asteroid lightcurve inversion: Ii. the complete inverse problem. *Icarus*, 153(1):37–51, 2001.
[20] J. G. Laframboise and J. Luo. High-voltage polar-orbit and beam-induced charging of a dielectric spacecraft: A wake-induced barrier effect mechanism. *Journal of Geophysical Research*, 94(A7):9033, 1989.
[21] Zhen Li, Marek Ziebart, Santosh Bhattarai, David Harrison, and Stuart Grey. Fast solar radiation pressure modelling with ray tracing and multiple reflections. *Advances in Space Research*, 61(9):2352–2365, 2018.
[22] M Martinez-Sanchez. Data Analysis for CHAWS Modeling. Technical report, Massachusetts Institute of Technology, 2000.
[23] Tomoko Matsuo, I-Te Lee, and Jeffrey L Anderson. Thermospheric mass density specification using an ensemble kalman filter. *Journal of Geophysical Research: Space Physics*, 118(3):1339–1350, 2013.
[24] Geoff McHarg, Parris Neal, Nikolas Taormina, Alex Strom, and Richard Balthazor. USAFA Integrated Miniaturized Electrostatic Analyzer (iMESA) - An Undergraduate Space Weather Constellation. *Space Weather*, 13(12):827–830, 2015.
[25] Denis Naughton, Robert Bedington, Simon Barraclough, Tanvirul Islam, Doug Griffin, Brenton Smith, Joe Kurtz, Andrey Alenin, Israel Vaughn, Arvind Ramana, Igor Dimitrijevic, Zong Sheng Tang, Christian Kurtsiefer, Alexander Ling, and Russell Boyce. Design considerations for an optical link supporting intersatellite quantum key distribution. *Optical Engineering*, 58(01):1, 2019.
[26] Steven G. Parker, James Bigler, Andreas Dietrich, Heiko Friedrich, Jared Hoberock, David Luebke, David McAllister, Morgan McGuire, Keith Morley, Austin Robison, and Martin Stich. OptiX: A general purpose ray tracing engine. *ACM SIGGRAPH*, 29(4), 2010.
[27] David Perez and Riccardo Bevilacqua. Lyapunov-Based Adaptive Feedback for Spacecraft Planar Relative Maneuvering via Differential Drag. *Journal of Guidance, Control, and Dynamics*, 37(5):1678–1684, 2014.
[28] David Pérez and Riccardo Bevilacqua. Neural Network Based Calibration of Atmospheric Density Models. *Acta Astronautica*, 110:58–76, 2015.
[29] David Pérez, Brendt Wohlberg, Thomas Alan Lovell, Michael Shoemaker, and Riccardo Bevilacqua. Orbit-Centered Atmospheric Density Prediction using Artificial Neural Networks. *Acta Astronautica*, 98(1):9–23, 2014.
[30] JM Picone, AE Hedin, D Pj Drob, and AC Aikin. Nrlmsise-00 empirical model of the atmosphere: Statistical

comparisons and scientific issues. *Journal of Geophysical Research: Space Physics*, 107(A12):SIA–15, 2002.
[31] M Cegarra Polo. Attitude detection of buccaneer rmm cubesat through experimental and simulated light curves in combination with telemetry data m. cegarra polo, r. abay, s. gehly, a. lambert, p. lorrain, s. balage, m. brown and c. bright. In *Advanced Maui Optical and Space Surveillance Technologies Conference, Maui, HI*, 2018.
[32] AD Richmond, EC Ridley, and RG Roble. A thermosphere/ionosphere general circulation model with coupled electrodynamics. *Geophysical Research Letters*, 19(6):601–604, 1992.
[33] Antonio Sanchez-Torres. Drag and propulsive forces in electric sails with negative polarity. *Advances in Space Research*, 57(4):1065–1071, 2016.
[34] Hanspeter Schaub, Gordon G Parker, and Lyon B King. Coulomb Thrusting Application Study. Technical report, Defence Advanced Research Projects Agency, 2006.
[35] B. G.A. Smith, C. J. Capon, M. Brown, and R. R. Boyce. Ionospheric drag for accelerated deorbit from upper low earth orbit. *Acta Astronautica*, 176(July):520–530, 2020.
[36] Brenton Smith. *A Comprehensive Examination of Low Earth Orbit Aerodynamic Accelerations for Satellite Formation Control*. PhD thesis, University of New Sourth Wales Canberra, 2019.
[37] Brenton Smith, Rasit Abay, Joshua Abbey, Sudantha Balage, Melrose Brown, and Russell Boyce. Propulsionless Planar Phasing of Miniaturised Satellites Using Deep Reinforcement Learning. In *International Workshop on Satellite Constellations and Formation Flying*, Glasgow, 2019.
[38] Brenton Smith, Russell Boyce, and Melrose Brown. Fast Aerodynamic Establishment of a Constellation of CubeSats. In *7th European Conference for Aeronautics and Space Sciences*, Milan, 2017.
[39] Brenton Smith, Russell Boyce, Melrose Brown, and Christopher Capon. Active use of ionospheric aerodynamics for the control of satellites. *42nd COSPAR Scientific Assembly*, 2018.
[40] Brenton Smith, Russell Boyce, Melrose Brown, and Matthew Garratt. An Investigation into the Practicability of Differential Lift Based Spacecraft Rendezvous. *Journal of Guidance, Control, and Dynamics.*, 40(10):2682–2689, 2017.
[41] Brenton Smith, Christopher Capon, and Melrose Brown. Ionospheric Drag for Satellite Formation Control. *Journal of Guidance, Control, and Dynamics*, 42(12):2590–2599, 2019.
[42] Nathan B Stastny, Frank R Chavez, Chin Lin, T Alan Lovell, Robert A Bettinger, and James Luck. Localized density/drag prediction for improved onboard orbit propagation. Technical report, AIR FORCE RESEARCH LAB KIRTLAND AFB NM SPACE VEHICLES DIRECTORATE, 2009.
[43] Nobie H Stone. The Aerodynamics of Bodies in a Rearefied Ionized Gas with Applications to Spacecraft Environmental Dynamics. Technical report, Marshall Space Flight Center, Alabama, 1981.
[44] Brett Streetman and Mason A Peck. New synchronous orbits using the geomagnetic lorentz force. *Journal of Guidance, Control, and Dynamics*, 30(6):1677–1690, 2007.
[45] Constantin Traub, Georg H. Herdrich, and Stefanos Fasoulas. Influence of energy accommodation on a robust spacecraft rendezvous maneuver using differential aerodynamic forces. *CEAS Space Journal*, 12(1):43–63, 2020.
[46] Hideyuki Usui, Yohei Miyake, Wojciech J. Miloch, and Keisuke Ito. Numerical Study of Plasma Depletion Region in a Satellite Wake. *IEEE Transactions on Plasma Science*, 47(8):3717–3723, 2019.
[47] J. Wang and D. E. Hastings. Ionospheric plasma flow over large high-voltage space platforms. I : lon-plasma-time scale interactions of a plate at zero angle of attack. *Phys. Fluids B*, 4(6):1597–1614, 1992.
[48] E C Whipple. Potentials of surfaces in space. *Reports on Progress in Physics*, 44(11):1197–1250, 1981.
[49] Olli Wilkman. Ray-tracer for modeling interactions of light with space objects. In *Advanced Maui Optical and Space Surveillance Technologies Conference*, 2018.